Influence of Pellet Shape of Ferro-Electric Packed-Bed Plasma Reactor on Ozone Generation and NO Removal

K. Takaki[1], S. Takahashi[1], S. Mukaigawa[1], T. Fujiwara[1], K. Sugawara[2] and T. Sugawara[2]
[1] Department of Electrical and Electronic Engineering, Iwate University, Japan
[2] Department of Materials-process Engineering and Applied Chemistry for Environments, Akita University, Japan

Abstract—An influence of pellet shape on performance of ferro-electric packed-bed plasma reactor for ozone generation and/or nitrogen monoxide (NO) removal was investigated experimentally. The plasma reactor consisted of a center metal rod electrode, glass tube and spherical or hollow cylindrical shaped ferro-electric pellets packed in the discharge area. Barium Titanate ($BaTiO_3$) was used as ferro-electric materials which had 10,000 dielectric constant. Pulse high voltage of 10 kV was applied to the center electrode with 1 kHz repetitive rate using a MOS-FET switch pulse generator. Aluminum tape was used as ground electrode and was wrapped around the glass tube. The ozone yield was improved by changing the pellet shape from sphere to hollow cylinder. NO removal efficiency also increased by changing pellet shape from sphere to hollow cylinder. In case of the spherical shaped pellet, the ozone generation and the NO removal of 3.3 mm diameter pellets showed higher efficiency than those of 2.4 mm diameter pellets.

Keywords—Packed-bed, Non-thermal plasma, Ferro-electric, Ozone, NO_x removal

I. INTRODUCTION

Packed bed dielectric barrier discharge plasma reactor has been widely investigated to remove the gaseous pollutants, such as particulate matter (PM), carbon dioxide (CO_2) [1], nitrogen oxides (NOx) [2-4], volatile organic compounds (VOCs) [5-12], hazardous air pollutants (HAPs) [13], perfluorocarbons (PFCs) [14-17], etc [18], from air or other gases. The packed bed plasma reactors are also utilized for ozone production in oxygen or dry air [19-22]. In this type of reactor, the electrical energy fed into the discharges is used preferentially to create energetic electrons instead of heating the ions and the neutral gas molecules [23, 24]. Especially, extremely high energetic electrons are produced near the contact points of ferroelectric pellets packed-in the plasma reactor [25-27], because of a huge electric field generated near the contact points [28, 29]. The energetic electrons are employed directly to dissociate and ionize the pollutants as well as carrier gas molecules to produce various radicals to react with and convert a part of pollutants.

Fundamental characteristics of a dielectric barrier discharge (DBD) in a ferro-electric packed bed reactor have been studied for the Barium Titanate ($BaTiO_3$) based spherical-shaped pellets for the specific dielectric constant from 660 to 10^4 from the viewpoint of reactor performance improvement [25, 30-32]. The dielectric constant of pellet packed in the reactor affects discharge characteristics such as power consumption of the reactor, microdischarge onset voltage, number of microdischarge. As the results, the performance of packed bed plasma reactor depends on the dielectric constant and/or material of the pellet packed in the reactor [33, 34]. The effect of pellet shape on the discharge characteristics has also been studied using three different shapes: spherical, cylindrical, hollow cylindrical pellets having the same specific dielectric constant 10^4. The experimental results showed the gas flow pressure drop of the packed-bed reactor could be reduced by changing the pellet shape from sphere to hollow cylinder [35]. The peak current of the microdischarge with the hollow cylindrical shaped pellets was much larger compared with the current of the spherical shaped pellets [35, 36]. The efficiency of C_2F_6 abatement increases with changing pellet shape from the sphere to the hollow-cylinder [36]. However, it is not clear that the change of discharge characteristics by the pellet shape affect the packed bed plasma reactor performance such as ozone generation or nitric oxide (NO) removal from gas streams.

This paper describes the influence of pellet shape packed in the plasma reactor on NO removal and ozone generation. Two different shapes; spherical and hollow cylindrical shaped $BaTiO_3$ pellets are used as ferro-electric material in the plasma reactor.

II. EXPERIMENTAL SETUP

Bench-scale ferro-electric packed-bed dielectric barrier discharge (PBDBD) plasma reactor is used in the experiment as shown in Figure 1. The plasma reactor consists of a center rod electrode (10 mm o.d.) and 2 mm thickness glass tube packed with $BaTiO_3$ pellets (Fuji Titanium Inc. MS-304) with dielectric constant of 10,000. The dimensions and physical properties of the pellets used in the packed bed reactor are summarized in

Corresponding author: Koichi Takaki
e-mail address: takaki@iwate-u.ac.jp

Presented at the 6th International Conference on Applied Electrostatics in November 2008, Accepted; March 6, 2009

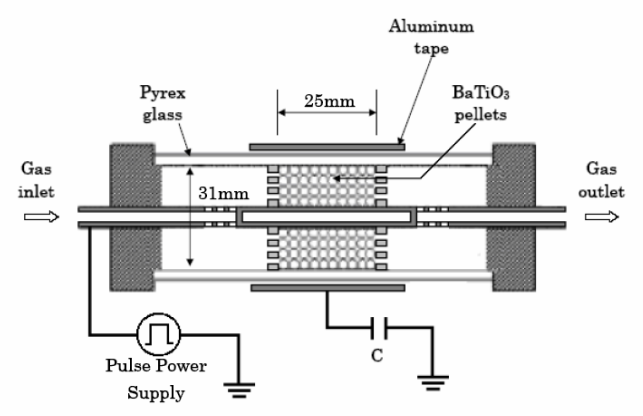

Fig.1. Schematic of the packed-bed reactor.

TABLE I
DIMENSIONS OF PELLET

Geometry	Size [mm]	Weight [g]	Void fraction
Sphere	diameter : 2.4	0.04	0.40
Sphere	diameter : 3.3	0.12	0.47
Hollow cylinder	o.d. 4.1, i.d. 1.7 length : 5	0.32	0.52

Table 1. The inner diameter of the glass tube is 31 mm i.e. 10 mm separation between the center electrode and the glass tube. The length of the discharge area is set to be 25 mm. The void fraction was measured using the reactor glass cylinder for the three different pellet shapes in random pack-in case. The void fraction was obtained as a ratio of total weight of the randomly packed in the reactor cylinder [g] to product of the reactor cylinder volume [ml] multiplied by pellet weight density [g/ml]. The void fraction of the hollow cylindrical pellets shows almost 1.3 times larger than that in other cases owing to inner hollow space.

Figure 2 shows equivalent circuit of the pulse modulator employed to drive the PBDBD plasma reactor [37]. The pulse modulator generates a square wave pulse with various duty factors. A three-phase 50 Hz sinusoidal voltage is rectified using a diode bridge. The rectified voltage is applied to a primary energy storage capacitor C. This part works as an AC/DC converter with maximum voltage of 300V. Four

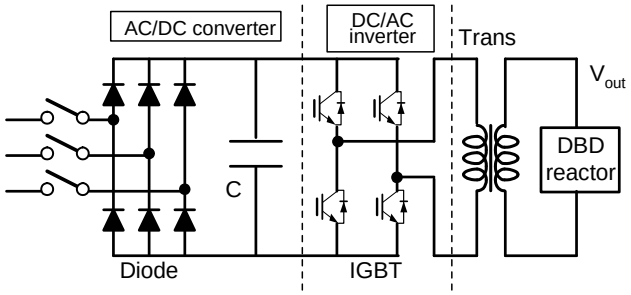

Fig.2. Equivalent circuit of pulse modulator for driving DBD reactor.

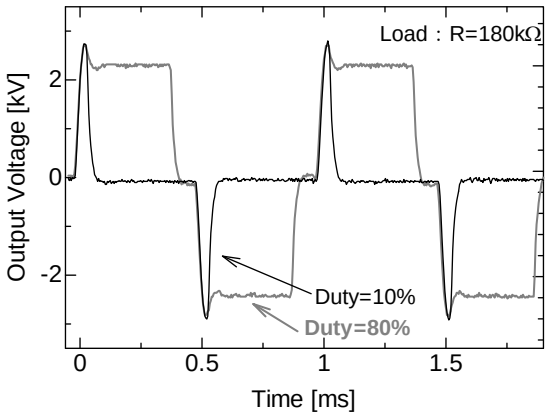

Fig.3. Typical waveforms output voltage of pulse modulator at two different pulse duty factors with 180 kΩ load resistor.

insulated gate bipolar transistor (IGBT) switches are used as repetitive closing switch to generate a square waveform voltage. This part is worked as DC/AC inverter. The pulse width i.e. the duty factor is controlled by timing of applying gate pulse to the IGBT switches. The pulse repetition rate is fixed at 1 kHz. The output voltage of 300 V is amplified to 10 kV using pulse transformer.

Figure 3 shows typical output voltage of the pulse modulator for two different pulse widths i.e. duty factors. A resistor of 180 kΩ is used as high impedance load in this case. The pulse width is successfully controlled from 50 to 400 μs i.e. from 10 to 80% of the duty factor, which is defined as ratio of pulse width to period of the output voltage.

The pulse high voltage was applied to the center electrode with 10% duty i.e. 50 μs pulse width by timing of gate signal applying to IGBT switches. Aluminum tape electrode surrounding the glass tube is connected to the ground. Tektronix model P6015 voltage probe is used to measure applied voltage. The charge accumulated on the dielectric materials is measured using a 0.01 μF capacitor inserted between the reactor and the ground. The signal was ob-served using a Tektronix TDS3054B digitizing oscilloscope with 500 MHz band width and 5 GS/s sampling rate. The consumed energy in the reactor is obtained using volt-age-charge curve (*V-Q* Lissajous figure).

The oxygen gas of 99.5% purity is used as source gas for the ozone generation with gas flow rate of 2.0 L/min. The ozone concentration was measured using Ebara EG-2001B Ozone Monitor at outlet of the reactor. For the NO removal experiment, 200 ppm NO diluted with gas mixture of nitrogen and oxygen with ratio of 9:1 is used as simulated diesel exhaust gas. The gas flow rate is also controlled to be 2.0 L/min using a mass flow controller. The concentration of NO was measured with a NOx analyzer (BEST Sokki BCL-511).

III. EXPERIMENTAL RESULT

A. Electrical discharge characteristics

Fig. 4 shows waveforms of applied voltage to the reactor and accumulated charge by microdischarges on

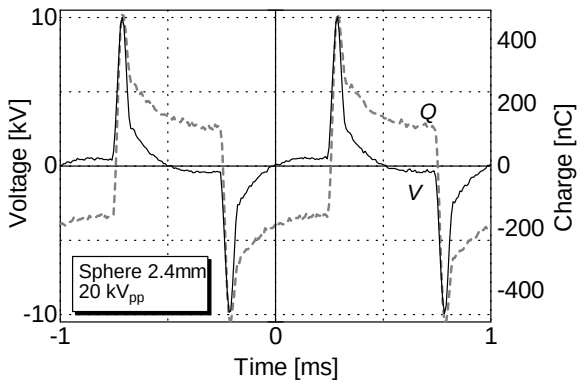

Fig. 4. Waveforms of applied voltage and accumulated charge by microdischarges on sphere pellets packed-bed reactor at 20 kV_{pp} applied voltage.

spherical pellets packed-bed reactor at 20 kV_{pp} (peak-to-peak voltage) applied voltage. The packed-bed DBD reactor generally works as a capacitive load. When the pulse voltage is applied, the DBD reactor worked as a capacitive load is charged up, as the result, a displacement current flow through the reactor. A large number of microdischarges also occur with high electric field. The charges of the microdischarges are accumulated on the surface of the pellets and the glass wall. Figure 4 clearly shows the charges are accumulated by applying pulse voltage to the reactor. From the observation using a Rogowski coil, the discharge current waveform of the microdischarges has several mAs to a few tens mA peak and around 10 ns of FWHM (full-width half maximum) pulse width [25]. The total movement charge by one microdischarge can be obtained with time-integration of the discharge current. The movement charges by one microdischarge are calculated to be 0.06 and 0.19 nC for spherical and hollow-cylindrical pellet, respectively. The total accumulated charge by half cycle of the applied voltage is obtained to be 340 nC as 153 nC at t=0.5 ms +187 nC at t=0. Therefore, several thousands of microdischarges are predicted to occur by applying one pulse voltage.

Figure 5 shows the *V*-*Q* Lissajous diagrams for two different pellet shapes at 20 kV_{pp} applied voltage. The areas of the two parallelograms shown in Fig. 5 are 4.7

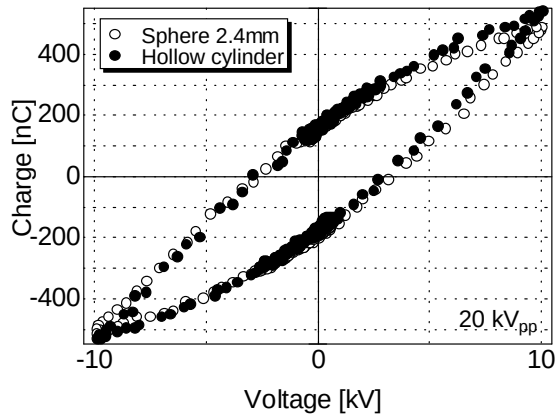

Fig. 5. *V*-*Q* Lissajous diagrams for two pellet shapes; the spherical and the hollow cylindrical shaped pellets at same 20 kV_{pp} applied voltage.

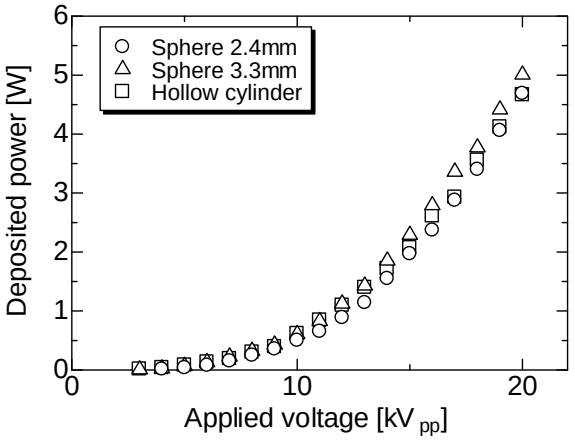

Fig. 6. Power deposition to the reactor as a function of applied voltage for various pellet shapes.

mJ for both cases. This value indicates the energy consumed in the PBDBD reactor per one applied voltage cycle [38, 39] and this 4.7 mJ energy corresponds to 4.7 W power deposited into the reactor under the present experimental condition. The accumulated charges with the discharges at the hollow cylindrical pellets are slightly larger than that of the spherical pellet, whereas the consumed energy with the hollow cylinder pellets is almost same with value of the sphere pellets.

Figure 6 shows deposited power in the reactor as a function of applied voltage for various pellet shapes. At low applied voltage smaller than 10 kV_{pp}, the deposited powers for three pellets are almost same, to be precise, the power for the hollow cylinder pellet is slightly larger than that for other shapes. However, the deposited power for the hollow cylinder pellets coincides with that of 3.3 mm diameter spherical pellets 10 kV_{pp}. At high-applied voltage larger than 10 kV_{pp}, the deposited power of the hollow cylinder pellets changes to lower than that 3.3 mm diameter spherical pellets.

B. Ozone generation

Figure 7 shows the generated ozone concentration as a function of applied voltage for three different pellet shapes. The ozone concentration increases with

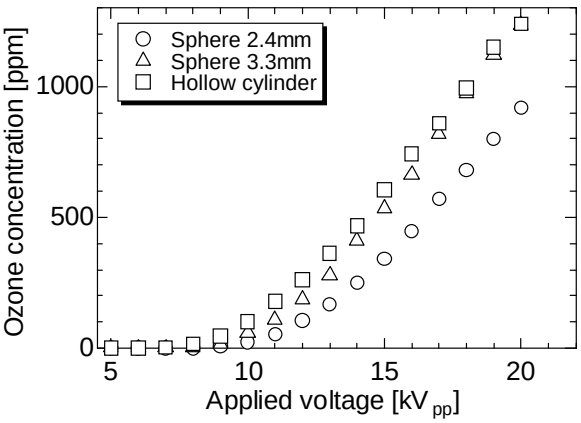

Fig. 7. Ozone concentration as a function of applied voltage for various pellet shapes.

increasing applied voltage at all pellet shape cases. However, the ozone generation depends on the pellet shape. The 1,240 ppm ozone is produced at hollow cylinder pellets and 20 kV_{pp} applied voltage. However, the ozone generation is only 920 ppm at 2.4 mm sphere pellet case.

Figure 8 shows the generated ozone concentration as a function of input (deposited) energy density to the plasma reactor for three different pellet dimensions. The input energy density to the reactor is obtained by the following equation,

$$w = \frac{60 \cdot U \cdot f}{q} \ , \qquad (1)$$

where U is energy consumed in the plasma reactor per one cycle of applied voltage, obtained from *V-Q* Lissajous diagram shown in Fig. 5. The symbols f and q mean the frequency of the applied voltage [Hz] and the gas flow rate [L/min.], respectively. Figure 8 indicates that ozone generation per input energy density depends on the pellet shape. The hollow cylinder pellet shows good performance for ozone generation among the three different pellet shapes. The ozone generation efficiency strongly depends on gas temperature [23]. From the observation using a thermocouple, the temperature in the plasma reactor increased with increasing input energy density. However, the temperature rise was lower than 10 Celsius and was almost independent of pellet shape under the experimental condition.

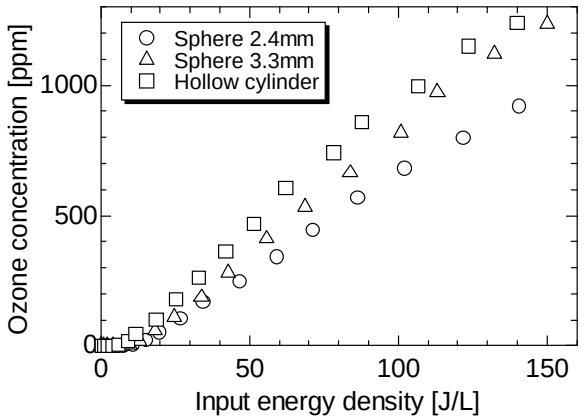

Fig. 8. Ozone concentration as a function of input energy density for various pellet shapes.

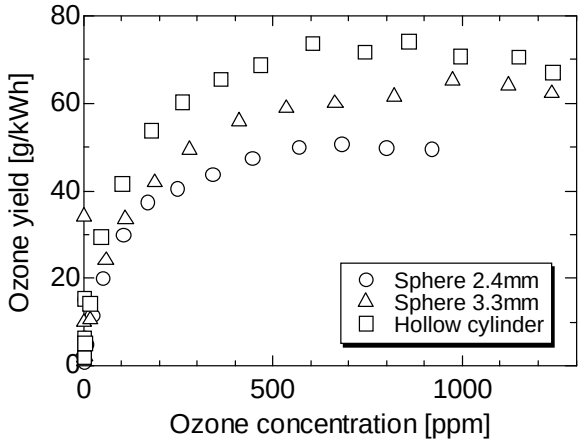

Fig. 9. Ozone yield as a function of ozone concentration for various pellet shapes.

Figure 9 shows the ozone yield as a function of generated ozone concentration for three different pellet shapes. The ozone yield is obtained by following equation,

$$\eta = \frac{60 \cdot q \cdot [O_3] \cdot M}{22.4 \cdot P} \times 10^{-3} \text{ [g/kWh]}, \qquad (2)$$

where $[O_3]$ is ozone concentration, M is molecular weight of ozone; 48, P is input power. Figure 9 indicates that the ozone yield changes by changing the pellet shape. The hollow cylinder pellet shows almost 73 g/kWh at 800 ppm ozone generation, while the 2.4 mm sphere and 3.3 mm sphere pellet show around 50 and 62 g/kWh, respectively.

C. NO removal

Figure 10 shows NO removal as a function of input energy density to the plasma reactor for three different pellet shapes. NO removal depends on the pellet shape. The hollow cylinder pellet also shows good performance for NO removal from simulated diesel exhaust gas among the three different pellet shapes. This dependence of the pellet shape on NO removal efficiency is almost same with the dependency for ozone generation as shown in Fig. 8. The almost NO is removed via oxidization processes such as;

$$O_3 + NO \rightarrow NO_2 \qquad (3)$$

$$O + NO + M \rightarrow NO_2 + M; \qquad (4)$$

under our experimental condition of 10% oxygen contained gas mixture [40]. Therefore, NO removal efficiency is estimated to depend on oxygen atoms generation rate. This is one of reason for the similar characteristics between the ozone generation and the NO removal.

Figure 11 shows the energy efficiency for NO removal as a function of NO removal for three different pellets. The energy efficiency for NO removal is obtained by following equation,

$$\eta = \frac{60 \cdot q \cdot \Delta[NO] \cdot M}{22.4 \cdot P} \times 10^{-3} \text{ [g/kWh]}, \qquad (5)$$

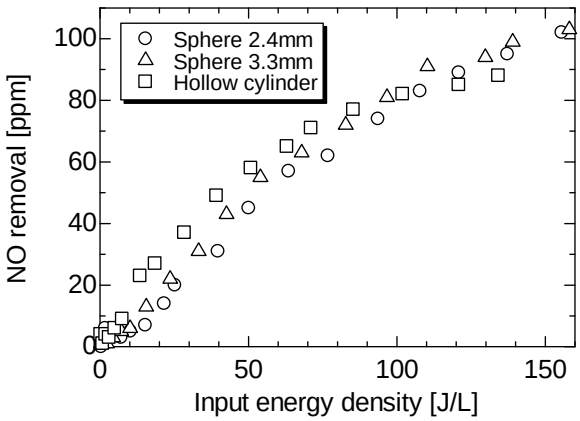

Fig. 10. NO removal as a function of input energy density for various pellet shapes.

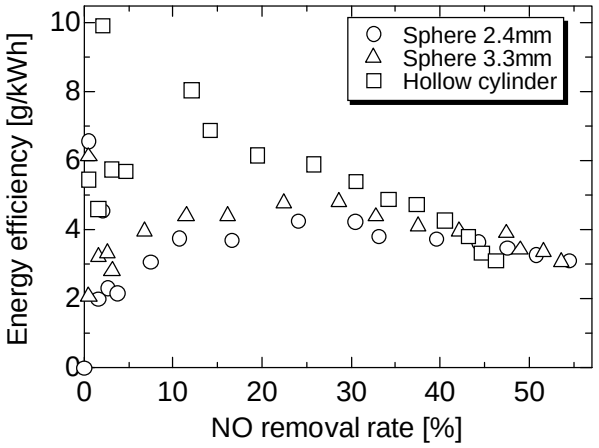

Fig. 11. Energy efficiency of NO removal as a function of ozone concentration for various pellet shapes.

where Δ[NO] is NO removal [ppm], *M* is molecular weight of NO; 30. The energy efficiency varies widely in lower NO removal than 10% owing to the microdischarge instability in the reactor at small input energy. Especially, the hollow cylinder pellet shows large scattering at the low NO removal rate because the hollow cylinder shape generates strongly distorted electric field distribution. Figure 11 indicates that energy efficiency slightly changed by changing the pellet shape. The hollow cylinder pellet shows almost 6.0 g/kWh at 25% NO removal, while the 2.4 mm sphere pellet shows 4.0 g/kWh. This result shows similar tendency with the ozone yield of 73 g/kWh for the hollow cylinder pellet and 50 g/kWh for the 2.4 mm sphere pellet. Therefore, the increase of the ozone yield by changing the pellet is main reason to the improvement of the NO removal efficiency by changing the pellet shape from sphere to the hollow cylinder.

V. DISCUSSIONS

A. Influence of pellet dielectric constant on ozone yield

The ferroelectric packed-bed plasma reactor was used for ozone generation and the ozone yield of 62 g/kWh was obtained at 3.3 mm diameter spherical pellets packed in the reactor. The obtained yield of 62 g/kWh is lower than values of 92 g/kWh at 3.0 mm diameter glass beads packed-in DBD reactor reported in ref. [22], and 105 g/kWh at 0.5-0.8 mm diameter quartz beads reported in ref. [20]. One of the reasons is predicted that the dielectric constant of the pellets packed in the DBD reactor strongly affects the ozone yield [41]. It was reported by J. Moon that the ozone yield decreased with increasing dielectric constant of the pellets in DBD reactor at larger dielectric constant of the pellets than 660 [41]. The electric field near the contact points of the pellets is changed with dielectric constant of the pellet. The microdischarges generate near the contact points. The electron energy and the power consumption of the microdischarges strongly depend on the electric field in the discharge. Therefore, the ozone yield strongly depends on dielectric constant of the pellets because the electron energy and the power consumption affect the ozone yield. In our experiment, the ferroelectric $BaTiO_3$ pellets with dielectric constant of 10,000 are packed in the reactor and the value of the dielectric constant is much larger than 660. Therefore, it is necessary to decrease the dielectric constant packed in the reactor in order to improve ozone yield.

Some researcher reported that the ozone yield increased by packing the pellet between a dielectric plane and an electrode. The ozone yield was improved from 80 to 91 g/kWh by packing silica pellets at 1.0 % ozone generation [19], from 14 to 173 g/kWh by packing alumina pellets [22]. This ozone yield increase is owing to the extremely high electric field near the contact points of the pellets [25]. The electrons are accelerated with the high electric field near the contact points and produce the atomic oxygen radicals. In our case, the ozone yield of 62 g/kWh is lower than that of conventional DBD ozonizer. Therefore, the improvement of the present packed bed plasma reactor is necessary, e.g. optimization of pellet material, for the industrial applications.

B. Influence of pellet shape on ozone yield

The hollow-cylindrical and the spherical shapes were employed as ferroelectric pellets packed in the reactor for ozone generation and the higher ozone yield of 70 g/kWh was obtained at hollow-cylindrical pellet shape as shown in Fig. 9. The characteristics of the microdischarges produced in the packed-bed plasma reactor are changed by pellet shape [36]. In general, by employing hollow-cylinder pellets the large number of microdischarges can be generated and the plasma reactor performance can be improved [36]. In the present experimental result also shows that the amount of movement charge with microdischarges in the hollow cylinder pellets packed reactor is about 1.07 μC (=540 + 530 nC) per one cycle of 20 kV_{pp} applied voltage as shown in Fig. 5. This value is larger than 0.99 μC (=490 + 500 nC) movement charge with microdischarges in the spherical pellets packed reactor where as the consumed energy per one cycle is same value of 4.7 mJ as shown in Fig. 6. As the results, time- and spatial-averaged electron density in the hollow cylinder pellets packed reactor is roughly estimated to be 8% larger value than that in the spherical pellets packed reactor at 20 kV_{pp} applied voltage. When ozone concentration is low enough to disregard the decomposition of ozone by O radicals such as $O(^1D)$, every dissociated oxygen atom is transformed into ozone molecules by the three-body collision reaction. These reactions are shown in equations (6)-(9) [42, 43].

$$e + O_2 \rightarrow O(^1D) + O + e \rightarrow O + O + e \quad (6)$$

$$e + O_2 \rightarrow O + O + e \quad (7)$$

$$e + O_2 \rightarrow O + O^- \quad (8)$$

$$O + O_2 + M \rightarrow O_3 + M \quad (9)$$

where M is the third collision partner; it takes part in energy absorption, but does not react chemically. Therefore, the number of generated oxygen atoms per one applied voltage cycle in the hollow cylinder pellets packed reactor estimated to be larger than that in the spherical pellets packed reactor with assumption of same reduced electric field.

VI. Conclusion

The ferro-electric packed-bed plasma reactor was experimentally investigated focusing with influence of ferro-electric pellet shape on performance of the reactor. The performance of the reactor was evaluated with ozone yield and the energy efficiency for NO removal from simulated diesel engine exhaust gas. The spherical and hollow cylindrical shaped $BaTiO_3$ pellets were used in the experiment and were packed in the discharge area. The packed-bed reactor with the hollow cylinder pellets generates the ozone with higher energy efficiency of 73 g/kWh than 50 g/kWh efficiency of the sphere pellets. NO removal also increased by changing pellet shape from sphere to hollow cylinder.

Acknowledgment

The author thanks Prof. J.S. Chang of McMaster University, Dr. K. Urashima of National Institute of Science and Technology Policy, Mr. Y. Sugawara of Akita Research and Development Center for their valuable comments and discussions. The author thanks Mr. Shida of Iwate University, Mr. H. Kobayashi of Akita University, Mr. T. Miura of Sawafuji Co. Ltd. for their technical supports. This work was supported by a Grant-In-Aid of Science Research from Japan Ministry of Education, Science and Culture (JSPS Fellowship No 18030001)

References

[1] K. Jogan, A. Mizuno, T. Yamamoto, and J. S. Chang, "The effect of residence time on the CO_2 reduction from combustion flue gases by an AC ferroelectric packed bed reactor," *IEEE Trans. Ind. Applicat.*, vol. 29, no. 5, pp. 876-881, 1993.

[2] T. Yamamoto, C. L. Yang, M. R. Beltran, and Z. Kravets, "Plasma-assisted chemical process for NOx control," *IEEE Trans. Ind. Applicat.*, vol. 36, no. 3, pp. 923-927, 2000.

[3] C. Fitzsimmons, J. T. Shawcross, and J. C. Whitehead, "Plasma-assisted synthesis of N_2O_5 from NO_2 in air at atmospheric pressure using a dielectric pellet bed reactor," *J. Phys. D: Appl. Phys.*, vol. 32, pp. 1136-1141, 1999.

[4] H. H. Kim, K. Takahashi, S. Katsura, and A. Mizuno, "Low-temperature NOx reduction pressures using combined systems of pulsed corona discharge and catalysts," *J. Phys. D: Appl. Phys.*, vol. 34, pp. 604-613, 2001.

[5] S. Futamura, A. H. Zhang, and T. Yamamoto, "The dependence of nonthermal plasma behavior of VOCs on their chemical structure," *J. Electrostatics*, vol. 42, pp. 51-62, 1997.

[6] A. Ogata, K. Mizuno, S. Kushiyama, and T. Yamamoto, "Methane decomposition in a barium titanate packed-bed nonthermal plasma reactor," *Plasma Chem. Plasma Process.*, vol. 18, no. 3, pp. 363-373, 1998.

[7] H. H. Kim, "Nonthermal plasma processing for air-pollution control: a historical review, current issues, and future prospects", *Plasma Process Polym.*, vol. 1, pp. 91-110, 2004.

[8] H. X. Ding, A. M. Zhu, X. F. Yang, C. H. Li, and Y. Xu, "Removal of formaldehyde from gas streams via packed-bed dielectric barrier discharge plasmas," *J. Phys. D: Appl. Phys.*, vol. 38, pp. 4160-4167, 2005.

[9] M. K. Park, C. G. Ryu, H. B. Park, H. W. Lee, K. C. Hwang, and C. H. Lee, "Decomposition of cyanogen chloride by using a packed bed plasma reactor at dry and wet air in atmospheric pressure," *Plasma Chem. Plasma Process.*, vol. 24, no. 1, pp. 117-136, 2004.

[10] C. H. Chang and T. S. Lin, "Decomposition of toluene and acetone in packed dielectric barrier discharge reactors," *Plasma Chem. Plasma Process.*, vol. 25, no. 3, pp. 227-243, 2005.

[11] Y. H. Song, S. J. Kim, K. I. Choi, and T. Yamamoto, "Effects of adsorption and temperature on a nonthermal plasma process for removing VOCs," *J. Electrostatics*, vol. 55, pp. 189-201, 2002.

[12] U. Roland, F. Holzer and F. -D. Kopinke, "Combination of non-thermal plasma and heterogeneous catalysis for oxidization of volatile organic compounds Part 2. Ozone decomposition and deactivation of γ-Al_2O_3," *Appl. Catal.B: Environ.*, vol. 58, no. 3, pp. 217-226, 2005.

[13] S. Futamura, A. Zhang, and T. Yamamoto, "Mechanisms for formation of inorganic byproducts in plasma chemical processing of hazardous air pollutants," *IEEE Trans. Ind. Applicat.*, vol. 35, no. 4, pp. 760-766, Aug. 1999.

[14] K Takaki, K. Urashima, and J. S. Chang, "Scale-up of ferro-electric packed bed plasma reactor for C_2F_6 decomposition," *Thin Solid Films*, vol. 506-507, pp. 414-417, 2006.

[15] K. Urashima, K. G. Kostov, J. S. Chang, Y. Okayasu, T. Iwaizumi, K. Yoshimura, and T. Kato, "Removal of C_2F_6 from a semiconductor process flue gas by a ferroelectric packed-bed barrier discharge reactor with an adsorbed," *IEEE Trans. Ind. Applicat.*, vol. 37, no. 5, pp. 1456-1463, Oct. 2001.

[16] M. B. Chang and S. J. Yu, "An atmospheric-pressure plasma process," *Environ. Sci. Technol.*, vol. 357, pp. 1587-1592, 2001.

[17] J. S. Chang, K. G. Kostov, K. Urashima, T. Yamamoto, Y. Okayasu, T. Kato, T. Iwaizumi, and K. Yoshimura, "Removal of NF_3 from semiconductor-process flue gas by tandem packed-bed plasma reactor and adsorbent hybrid systems," *IEEE Trans. Ind. Applicat.*, vol. 36, no. 5, pp. 1251-1259, Oct. 2000.

[18] A. Mizuno, Y. Yamazaki, H. Ito, and H. Yoshida, "ac energized ferroelectric pellet bed gas cleaner," *IEEE Trans. Ind. Applicat.*, vol. 28, no. 3, pp. 535-540, June 1992.

[19] K. S. Szalowski and A. Borucka, "Heterogeneous effects in the process of ozone synthesis in electrical discharges," *Plasma Chem. Plasma Process.*, vol. 9, no. 2, pp. 235-255, 1989.

[20] K. S. Szalowski, "Catalytic properties of silica packings under ozone synthesis conditions," *Ozone Sci. Eng.*, vol. 18, pp. 41-55, 1996.

[21] S. Jodzis, "Effect of silica packing on ozone synthesis from oxygen-nitrogen mixture," *Ozone Sci. Eng.*, vol. 25, pp. 63-72, 2003.

[22] H. L. Chen, H. M. Lee, and M. B. Chang, "Enhancement of energy yield for ozone production via packed-bed reactors," *Ozone Sci. Eng.*, vol. 28, pp. 111-118, 2006.

[23] B. Eliasson and U. Kogelschatz, "Nonequilibrium volume plasma chemical processing," *IEEE Trans. Plasma Sci.*, vol. 19, no. 6, pp. 1063-1077, Dec. 1991.

[24] J. S. Chang, P. A. Lawless, and T. Yamamoto, "Corona discharge process," *IEEE Trans. Plasma Sci.*, vol. 19, no. 6, pp. 1152-1166, Dec. 1991.

[25] K Takaki, J. S. Chang, and K. G. Kostov, "Atmospheric pressure nitrogen plasmas in a ferro-electric packed bed barrier discharge reactor Part I: Modelling," *IEEE Trans. Diel. Elect. Insul.*, vol. 11, no. 3, pp. 481-490, June 2004.

[26] W. S. Kang, J. M. Park, Y. Kim, and S. H. Hong, "Numerical study on influences of barrier arrangements on dielectric barrier discharge characteristics," *IEEE Trans. Plasma Sci.*, vol. 31, no. 4, pp. 504-510, Aug. 2003.

[27] A. Ohsawa, R. Morrow, and A. B. Murphy, "An investigation of a de dielectric barrier discharge using a disc of glass beads," *J. Phys. D: Appl. Phys.*, vol. 33, pp. 1487-1492, 2000.

[28] Y. Nakajima and T. Matsuyama, "Electrostatic field and force calculation for a chain of identical dielectric spheres aligned parallel to uniformly applied electric field," *J. Electrostatics*, vol. 55, pp. 203-221, 2002.

[29] T. Takuma, "Field behavior at a triple junction in composite dielectric arrangements," *IEEE Trans. Elect. Insul.*, vol. 26, no. 3, pp. 500-509, June 1991.

[30] A. Mizuno and H. Ito, "Basic performance of an electrostatically augmented filter consisting of a packed ferroelectric pellet layer," *J. Electrostatics*, vol. 25, pp. 97-107, 1990.
[31] T. Kawasaki, S. Kanazawa, T. Ohkubo, J. Mizeraczyk, and Y. Nomoto, "Dependence of sintering temperatures of the $BaTiO_3$ pellets on N_2O generation characteristics in a packed-bed plasma reactor," *Thin Solid Films*, vol. 386, pp. 177-182, 2001.
[32] Y. Uchida, K. Takaki, K. Urashima, and J. S. Chang, "Atmospheric pressure nitrogen plasmas in a ferro-electric packed bed barrier discharge reactor part II: Spectroscopic measurements of excited molecule density and vibrational temperature," *IEEE Trans. Diel. Elect. Insul.*, vol. 11, no. 3, pp. 491-497, June 2004.
[33] A. Ogata, N. Shintani, K. Mizuno, S. Kushiyama, and T. Yamamoto, "Decomposition of benzene using a nonthermal plasma reactor packed with ferroelectric pellets," *IEEE Trans. Ind. Applicat.*, vol. 35, no. 4, pp. 753-759, Aug. 1999.
[34] F. Holzer, F.D. Kopinke and U. Roland, "Influence of ferroelectric materials and catalysts on the performance of non-thermal plasma (NTP) for the removal of air pollutants," *Plasma Chem. Plasma Process.*, vol. 25, no. 6, pp. 595-611, 2005.
[35] J. S. Chang, A. Chakrabarti, K. Urashima, and M. Arai, "The effect of barium titanium pellet shapes on the gas discharge characteristics of ferroelectric packed bed reactors", *Annual Report of 1998 Conf. on Electrical Insulation and Dielectric Phenomena*, pp. 485-488, 1998.
[36] K. Takaki, K. Urashima, and J. S. Chang, "Ferro-electric pellet shape effect on C_2F_6 Removal by a packed bed type non-thermal plasma reactor," *IEEE Trans. Plasma Sci.*, vol. 32, no. 6, pp. 2175-83, Dec. 2004.
[37] T. Miura, T. Sato, K. Arima, S. Mukaigawa, T. Takaki, and T. Fujiwara, "Duty Factor Effect on Ozone Production Using Dielectric Barrier Discharge Reactor Driven by IGBT Pulse Modulator," *J. Adv. Oxid. Technol.*, vol. 10, no. 2, pp. 311-315, July 2004.
[38] K. Takaki and T. Fujiwara, "Multipoint Barrier Discharge Process for Removal of NOx from Diesel Engine Exhaust," *IEEE Trans. Plasma Sci.*, vol. 29, no. 3, pp. 518-523, June 2001.
[39] K. Takaki, M. Shimizu, S. Mukaigawa, and T. Fujiwara, "Effect of Electrode Shape in Dielectric Barrier Discharge Plasma Reactor for NOx Removal," *IEEE Trans. Plasma Sci.*, vol. 32, no. 1, pp. 32-38, Feb. 2004.
[40] K. Takaki, M. A. Jani, and T. Fujiwara, "Removal of nitric oxide in flue gases by multipoint to plane dielectric barrier discharge," *IEEE Trans. Plasma Sci.*, vol. 27, no. 4, pp. 1137-1145, Aug. 2001.
[41] J. D. Moon and S. T. Geum, "Discharge and Ozone Generation Characteristics of a Ferroelectric-Ball/Mica-Sheet Barrier," *IEEE Trans. Elect. Insul.*, vol. 34, no. 6, pp. 1206-1211, Nov. 1998.
[42] J. Kitajima and M. Kuzumoto, "Analysis of ozone generation from air in silent discharge," *J. Phys. D: Appl. Phys.*, vol. 32, pp. 3032-3040, 1999.
[43] B. Eliasson, M. Hirth, and U. Kogelschatz, "Ozone synthesis from oxygen in dielectric barrier discharges," *J. Phys. D: Appl. Phys.*, vol. 20, pp. 1421-1437, 1987.